

Note

Despinning plus global contraction and the orientation of lobate scarps on Mercury: Predictions for MESSENGER

Andrew J. Dombard^{a,*}, Steven A. Hauck II^b

^a The Johns Hopkins University Applied Physics Laboratory, 11100 Johns Hopkins Road, Laurel, MD 20723, USA

^b Department of Geological Sciences, Case Western Reserve University, 10900 Euclid Avenue, Cleveland, OH 44106, USA

ARTICLE INFO

Article history:

Received 8 February 2008

Revised 5 June 2008

Available online 3 July 2008

Keywords:

Mercury

Interiors

Tectonics

Thermal histories

ABSTRACT

Observations by the Mariner 10 spacecraft suggest that the lobate scarps on Mercury, which have been interpreted to record at most 1–2 km of radial contraction of the planet after the end of the Late Heavy Bombardment, possess a global, preferred N–S orientation but lack a strong latitudinal dependence on their surface expression. Here, we reexamine the idea that a decrease in the planetary rotation rate (despinning) coupled with global contraction of at least 3–5.5 km prior to the end of Late Heavy Bombardment resulted in global N–S oriented thrust faults. The surface expression of these faults is assumed to have been erased by the end of the Late Heavy Bombardment, and the faults were subsequently reactivated by later global contraction, producing generally N–S oriented thrust faults from an isotropic stress field. We use the estimate of >3–5.5 km contraction prior to ~4 Ga as an additional constraint to thermomechanical simulations of the evolution of Mercury, finding that a wide range of models are consistent with this observation. The fact that a wide range of states are consistent with the contraction of Mercury prior to the end of Late Heavy Bombardment but only a restricted set of states are consistent with the at most 1–2 km of subsequent contraction bolsters the idea that there may be hidden strain on Mercury, features unseen by Mariner 10 but likely visible to the MESSENGER spacecraft.

© 2008 Elsevier Inc. All rights reserved.

1. Introduction

Mercury is the least imaged and hence least understood of the terrestrial planets. (That view, however, is changing; as of the writing of this article, NASA's MESSENGER spacecraft had completed the first of 3 flybys before it enters into orbit around Mercury in 2011.) Images from three flybys by NASA's Mariner 10 spacecraft back in the 1970's revealed a network of lobate scarps on the ~45% of the surface that was viewable; these structures (Fig. 1) are linear to arcuate, tens to hundreds of kilometers in length with relief up to a few kilometers, and are inferred to be the surface expression of large thrust faults (Strom et al., 1975). Given the ubiquitous nature of the lobate scarps on the portion observed by Mariner 10 of the surface and the lack of extensional features, the scarps have been interpreted to record at most 1–2 km of radial contraction associated with cooling of the planet over the last ~4 Gyr (i.e., since the end of Late Heavy Bombardment [LHB]; Strom et al., 1975; Watters et al., 1998). We have previously used this range as a constraint in models of the thermomechanical evolution of Mercury, generally predicting more radial contraction over the last 4 Gyr than is observed and only satisfying the constraint of limited contraction for a restricted set of parameters: a dry olivine-dominated mantle, heat production provided primarily by the decay of Th, and a bulk core sulfur content >6.5 wt% (Hauck et al., 2004).

A somewhat enigmatic observation is that the lobate scarps may be preferentially oriented N–S (Melosh and McKinnon, 1988, and references therein; Watters et al., 2004). While there is a spread in the orientations (Watters et al., 2004) and orientations of individual scarps may be locally influenced by mechanical discontinuities (e.g., impact basins; Watters et al., 2001), N–S preferentially oriented lobate scarps are difficult to reconcile with a shrinking planet. Global contraction would produce an isotropic stress field on the surface, resulting in tectonic structures with no preferred orientation. Consequently, it has been pro-

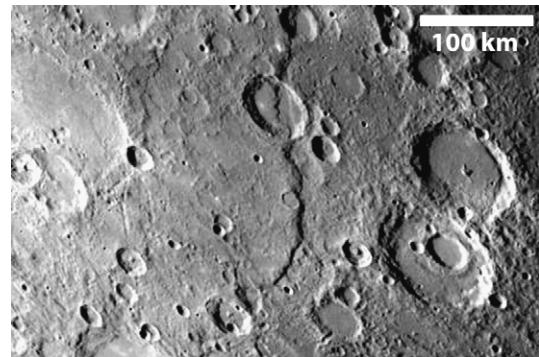


Fig. 1. This image from Mariner 10 shows an approximately 350-km long section of Discovery Rupes. The transected craters in the upper center of the image are ~35 and 55 km across; this larger crater lies at approximately -54° N, 38° W. Image PIA02446 from the NASA Planetary Photojournal (<http://photojournal.jpl.nasa.gov>); courtesy NASA/JPL-Caltech.

posed that global contraction augmented by stresses associated with despinning of the planet could yield N–S-oriented thrust faulting (Melosh and Dzurisin, 1978; Pechmann and Melosh, 1979). Here, we resurrect this idea and use it to provide an additional constraint to our thermomechanical models.

2. Global contraction plus despinning

The stress field from global contraction of a planet can be predicted with a simple thin-elastic-shell model of a planet:

$$\sigma_{\text{lon}} = \sigma_{\text{lat}} = \frac{E \Delta r}{1 - \nu r}, \quad (1)$$

* Corresponding author at: Department of Earth and Environmental Sciences (MC-186), University of Illinois at Chicago, 845 W. Taylor Street, Chicago, IL 60607-7059, USA. Fax: +1 312 413 2279.

E-mail address: adombard@uic.edu (A.J. Dombard).

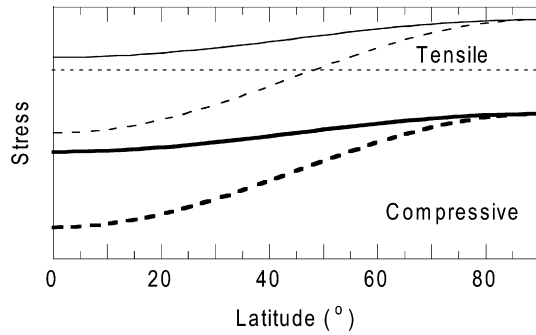


Fig. 2. Schematic representation of stresses from a thin-elastic-shell model for despinning (thin lines) and despinning plus global contraction (thick lines); the dotted line divides compressive and tensile stress regimes. For each set, the longitudinal (E–W) stress (dashed curves) is always more compressive than the latitudinal (N–S) stress (solid curves). For despinning only, stresses in polar regions are tensile and favor the development of E–W normal faults. With sufficient global contraction, the tensile despinning stresses can be driven to compressive failure, favoring the global development of N–S thrust faults.

where σ_{lon} and σ_{lat} are the stresses in longitudinal (E–W) and latitudinal (N–S) directions, E and ν are the Young’s modulus and Poisson’s ratio, r is the radius of the planet, and Δr is the change in radius (see Melosh and McKinnon, 1988). (Negative stresses are compressional.) Clearly, the stresses are equal across the surface, which would not favor a preferred orientation to any resultant tectonics.

A simple, thin-elastic-shell model can also be used to predict stresses of a despinning planet (see Melosh and McKinnon, 1988, from a derivation originally presented by Vening-Meinesz, 1947):

$$\sigma_{lon} = -\frac{5}{24} \Delta m \frac{E}{5 + \nu} (1 + 9 \cos 2\theta), \quad (2a)$$

$$\sigma_{lat} = \frac{5}{24} \Delta m \frac{E}{5 + \nu} (5 - 3 \cos 2\theta), \quad (2b)$$

where θ is latitude, and Δm is the difference between the initial and final ratios of the centripetal acceleration at the equator to gravitational acceleration, which is given by

$$\Delta m = \frac{(\Omega_0^2 - \Omega_f^2)r^3}{GM}. \quad (3)$$

Here, Ω_0 and Ω_f are the initial and final angular rotation rates (2π over the rotational period), M is the mass of Mercury, and G is the universal gravitational constant. These equations predict (Fig. 2) tensile stresses in polar regions, with the magnitude of the latitudinal stress exceeding the longitudinal stress such that a resultant tectonic feature would be an E–W striking normal fault. The magnitudes of the stresses are identical at the poles and become more compressive as the equator is approached. Thus, addition of an isotropic compressive stress field (e.g., from global contraction) of sufficient magnitude would add to the despinning stresses to produce global thrust faults, oriented N–S because the longitudinal stresses would always be more compressive than the latitudinal stress (Fig. 2). We can place a lower bound on the magnitude of the necessary decrease in planetary radius by calculating the compressive stress needed to overcome the maximum tensile stresses from despinning (i.e., at the poles) and then take the lithosphere to compressive failure.

The resultant stress field would predict stronger compressive stresses near the equator, and hence better developed lobate scarps at low latitudes. This is not observed in the Mariner 10 images; if anything, the lobate scarps may be better expressed at high southern latitudes (Watters et al., 2004). The despinning time scale for Mercury has been estimated to be <1 Gyr (Melosh and McKinnon, 1988). Thus, one plausible explanation for the lack of a strong latitudinal dependence to the lobate scarps is that despinning (plus contraction) occurred prior to the end of LHB. The surface expression of the initial scarps was erased, and the presently observed scarps arose from an isotropic, global-contraction stress field that reactivated pre-existing faults, thus inheriting a preferred N–S orientation but without developing a strong latitudinal dependence on the expression of the scarps. Because of the lack of a strong dependence on latitude, we assume that despinning occurred prior to ~ 4 Ga, and thus, we can estimate the magnitude of an early phase of global contraction by determining the magnitude of contraction that is needed to predict global, N–S oriented thrust faults when combined with despinning stresses.

Mercury’s current sidereal rotational period is ~ 59 days, down from an estimated initial period of ~ 20 h (see Melosh and McKinnon, 1988). We use measured values for the mass and mean radius of Mercury and assume a canonical value of Poisson’s ratio (0.25) and a Young’s modulus of 100 GPa (Turcotte and Schubert, 1982). The amount of contraction is dependent on the strength of faults. This value has been estimated for large faults on the Earth, Mars, and Venus to span the range of ~ 10 – 80 MPa (Barnett and Nimmo, 2002). Using these values, ~ 3.1 – 4.4 km of

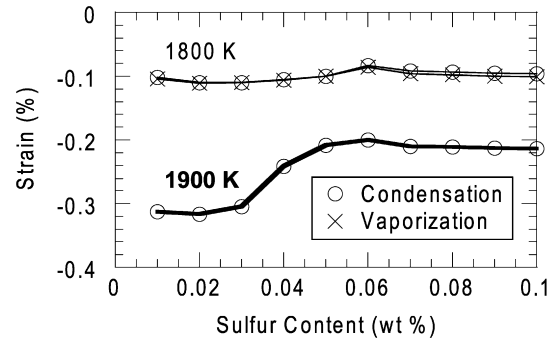


Fig. 3. Thermomechanical model results, showing integrated surface strain pre-4 Ga as a function of bulk core sulfur content. The thin curves show results from cases with an initial upper-mantle temperature of 1800 K, while the thick curve is for a temperature of 1900 K. The curves identified with circles depict cases where the heat-producing elements are consistent with a condensation-sequence-dominated assemblage (rich in U and Th with negligible K), while the curve with X’s are consistent with a late-stage silicate vaporization model for the high metal content of Mercury, with high Th but depleted in U and K (see Hauck et al., 2004).

global contraction is predicted. Allowing a reasonable 40% variation in the Young’s modulus of the elastic lithosphere of Mercury expands this range to ~ 3 – 5.5 km of global contraction prior to ~ 4 Ga. This range of values represents a lower bound to the amount of global contraction of Mercury prior to the end of the LHB.

3. Thermomechanical model

Our approach to understanding Mercury’s global contraction (or expansion) is to couple a model for the planet’s internal thermal evolution to a model for the accumulation of thermoelastic strains in an elastic shell overlying an inviscid interior (see Hauck et al., 2004, and references therein for complete details); the model runs presented here are identical to those in our previous work, except we now track the accumulation of horizontal strains at the surface prior to the end of the LHB (pre-4 Ga). The thermal model calculates both the convective and conductive parts of the heat lost through the lithosphere and mantle, the cooling of the core and solidification of an inner core, and the production of melt and formation of a crust. We implement a parameterized mantle convection technique, using a Rayleigh–Nusselt number relationship for fluids with strongly temperature-dependent viscosities, and modified to include the potential transition to full conduction. By employing a one-dimensional representation of convective heat transfer in a spherical shell overlying a core, coupled to a finite-element model for conduction in the lithosphere (and the mantle if convection ceases), we can calculate representative thermal evolution scenarios for the planet (Hauck et al., 2004). Overall, planetary cooling and precipitation of a solid iron inner core result in changes in planetary volume, which are recorded in the lithosphere through an accumulation of horizontal strains. The thickness of the elastic lithosphere is defined by the depth to the 950-K isotherm.

4. Results

We have previously used estimates of the amount of strain recorded in lobate scarps as a constraint on the internal evolution of Mercury over the last 4 Gyr (Hauck et al., 2004). In contrast, here we estimate the amount of contraction in our thermal evolution models during the first ~ 0.5 Gyr of the planet’s history. The rate of radial contraction of Mercury due to planetary cooling depends primarily on the initial temperatures of the interior, the viscosity of the mantle, the abundance of heat producing elements, and the amount of a light, alloying element in the core. Most simulations result in comparable amounts of post-4.0 Ga global contraction in excess of the at most 1–2 km currently recorded by the lobate scarps, except for one suite in which the high metal-to-silicate ratio of Mercury is a product of silicate vaporization, with heat production provided only by long-lived (14 -Gyr half-life) ^{232}Th , a dry olivine-dominated mantle, and a bulk core sulfur content >6.5 wt%.

To utilize our estimate of pre-4 Ga contraction of ~ 3 – 5.5 km as an additional constraint, we have recalculated a select subset of simulations to determine the amount of strain (i.e., radial contraction) that is generated before the end of LHB. Three suites of simulations, two with heat-producing-element compositions dominated by a condensation-sequence assemblage but with differing initial interior temperatures (1800 and 1900 K), and one with heat production constrained by a vaporization model (1800 K initial temperature) are calculated. Fig. 3 illustrates the amount of contractional strain accumulated in the first ~ 0.5 Gyr of the planet’s history as a function of bulk core sulfur content for each of these three suites. The two simulations with initial upper-mantle temperatures of 1800 K achieve $\sim 0.1\%$ contractional strain (i.e., ~ 2 – 3 km of radial contraction) and are virtually indistinguishable despite the $>30\%$ higher heat production in the vaporization-based model during this period. This result suggests insensitivity to heat production in this earliest period as the evolution is driven by shedding of the initial heat content of the

planet related to its formation and differentiation. It is also evident from Fig. 3 that the amount of global contraction is very sensitive to the initial temperatures of the interior, as an increase of 100 K leads to at least an additional 2–2.5 km of contraction. Thus, our simulations are consistent with this lower bound on the pre-4 Ga contraction of Mercury as long as the initial interior temperature was sufficiently high. The notion that the initial upper-mantle temperature was ~ 1900 K or higher also provides further evidence for a significant amount of sulfur in the core, because initially warmer, low-sulfur models experience more post-4 Ga contraction than is recorded in the observed lobate scarps (cf. Fig. 5 in Hauck et al., 2004).

5. Discussion

Our results suggest that a wide range of models for the thermal evolution of Mercury's interior may be consistent with the idea that early despinning of the planet with concurrent global contraction could be responsible for a N–S preference in lobate scarp orientation. That the amount of radial contraction in the first ~ 0.5 Gyr is strongly sensitive to initial temperatures of the interior is not entirely surprising, because hotter interiors will have lower mantle viscosities and thus more vigorous mantle convection, and can cool quickly toward quasi-equilibrium with heat output. Interestingly, these results also include those simulations that are the closest to being consistent with the post-4.0 Ga accumulation of strain (Hauck et al., 2004). This observation, however, raises an intriguing question: why is it relatively simple to generate thermal history models that satisfy the strain constraints provided by despinning in the first ~ 0.5 Gyr of Mercury's history, but finding reasonable models that match the post-4.0 Ga constraint requires either extraordinary compositions or considerably more strain than is recorded in the lobate scarps imaged by Mariner 10?

Data that have and will be obtained by the MESSENGER mission to Mercury (Solomon et al., 2007) will be critical for testing and refining our main hypothesis. A primary test will be a more robust determination of the somewhat contentious notion (Melosh and McKinnon, 1988; Watters et al., 2004) that there is, in fact, a preferred orientation to the lobate scarps. Furthermore, MESSENGER may discover that there is a strong latitudinal dependence to the surface expression of the lobate scarps. Determination of a lack of a preferred N–S orientation or the presence of a strong latitudinal dependence will require re-evaluation of the ideas discussed in this article.

If the Mariner 10 observations hold up, however, then the notion that a wide range of states are consistent with the contraction of Mercury prior to the end of LHB but only a restricted set of states are consistent with subsequent contraction buttresses the idea that additional contractional strain is recorded in the lithosphere. There are several possibilities for this “hidden” strain: long-wavelength, low-amplitude folds (Dombard et al., 2001), pervasive, small-scale faulting not resolved by Mariner 10 (Strom et al., 1975), or more intense faulting in the $\sim 55\%$ of the surface not seen by Mariner 10. MESSENGER is well poised to explore these possibilities. The global Mercury Dual Imaging System (MDIS) imagery (Hawkins et al., 2007), which is better optimized for morphometric analysis, and topographic data

(from MDIS stereo images and Mercury Laser Altimeter ranges; Cavanaugh et al., 2007) can be used to search for this hidden strain (and estimate better the amount of strain recorded in the lobate scarps). Lack of additional tectonism would support a very restricted composition for Mercury's interior (e.g., Hauck et al., 2004); however leveraging the axiom of Occam's razor, it seems likely that MESSENGER will uncover this hidden strain.

Acknowledgments

We thank Sean C. Solomon and Roger J. Phillips for helping to shape our ideas about Mercury, and we wish great luck to the entire MESSENGER team. Reviews by H. Jay Melosh and Thomas R. Watters helped us refine our arguments.

References

- Barnett, D.N., Nimmo, F., 2002. Strength of faults on Mars from MOLA topography. *Icarus* 157, 34–42.
- Cavanaugh, J.F., and 18 colleagues, 2007. The Mercury Laser Altimeter instrument for the MESSENGER mission. *Space Sci. Rev.* 131, 451–479.
- Dombard, A.J., Hauck II, S.A., Solomon, S.C., Phillips, R.J., 2001. Potential for long-wavelength folding on Mercury. *Lunar Planet. Sci.* 32. Abstract 2035.
- Hauck II, S.A., Dombard, A.J., Phillips, R.J., Solomon, S.C., 2004. Internal and tectonic evolution of Mercury. *Earth Planet. Sci. Lett.* 222, 713–728.
- Hawkins, S.E., and 24 colleagues, 2007. The Mercury dual imaging system on the MESSENGER spacecraft. *Space Sci. Rev.* 131, 247–338.
- Melosh, H.J., Dzurisin, D., 1978. Mercurian global tectonics: A consequence of tidal despinning? *Icarus* 35, 227–236.
- Melosh, H.J., McKinnon, W.B., 1988. The tectonics of Mercury. In: Vilas, F., Chapman, C.R., Matthews, M.S. (Eds.), *Mercury*. Univ. of Arizona Press, Tucson, pp. 374–400.
- Pechmann, J.B., Melosh, H.J., 1979. Global fracture patterns of a despun planet: Application to Mercury. *Icarus* 38, 243–250.
- Solomon, S.C., McNutt Jr., R.L., Gold, R.E., Domingue, D.L., 2007. MESSENGER mission overview. *Space Sci. Rev.* 131, 3–39.
- Strom, R.G., Trask, N.J., Guest, J.E., 1975. Tectonism and volcanism on Mercury. *J. Geophys. Res.* 80, 2478–2507.
- Watters, T.R., Robinson, M.S., Cook, A.C., 1998. Topography of lobate scarps on Mercury: New constraints on the planet's contraction. *Geology* 26, 991–994.
- Watters, T.R., Cook, A.C., Robinson, M.S., 2001. Large-scale lobate scarps in the southern hemisphere of Mercury. *Planet. Space Sci.* 49, 1523–1530.
- Watters, T.R., Robinson, M.S., Bina, C.R., Spudis, P.D., 2004. Thrust faults and the global contraction of Mercury. *Geophys. Res. Lett.* 31, doi:10.1029/2003GL019171. L04701.
- Turcotte, D.L., Schubert, G., 1982. *Geodynamics: Applications of Continuum Physics to Geological Problems*. Wiley, New York, 450 pp.
- Vening-Meinesz, F.A., 1947. Shear patterns of the Earth's crust. *Trans. AGU* 28, 1–61.